Neutron spectroscopic factors of ^{7}Li and astrophysical ^{6}Li(n,γ)^{7}Li reaction rates *

SU Jun,† LI Zhi-Hong, GUO Bing,
BAI Xi-Xiang, LI Zhi-Chang, LIU Jian-Cheng, WANG You-Bao, LIAN Gang, ZENG Sheng,
WANG Bao-Xiang, YAN Sheng-Quan, LI Yun-Ju, LI Er-Tao, FAN Qi-Wen, and LIU Wei-Ping
China Institute of Atomic Energy, P. O. Box 275(46), Beijing 102413, P. R. China

Angular distributions of the ^{7}Li(^{6}Li,^{6}Li)^{7}Li elastic scattering and the ^{7}Li(^{6}Li,^{7}Li$_{g.s.}$)^{6}Li, ^{7}Li(^{6}Li,^{7}Li$_{0.48}$)^{6}Li transfer reactions at E$_{c.m.}$=23.7 MeV were measured with the Q3D magnetic spectrograph. The optical potential of ^{6}Li+^{7}Li was obtained by fitting the elastic scattering differential cross sections. Based on the distorted wave Born approximation (DWBA) analysis, spectroscopic factors of ^{7}Li=^{6}Li⊗n were determined to be 0.73 ± 0.05 and 0.90 ± 0.09 for the ground and first exited states in ^{7}Li, respectively. Using the spectroscopic factors, the cross sections of the ^{6}Li(n,$\gamma_{0,1}$)^{7}Li direct neutron capture reactions and the astrophysical ^{6}Li(n,γ)^{7}Li reaction rates were derived.

PACS numbers: 21.10.Jx, 25.60.Bx, 25.60.Je, 26.35.+c

Recently, lithium isotopes have attracted an intense interest because the abundance of both ^{6}Li and ^{7}Li from big bang nucleosynthesis (BBN) is one of puzzles in nuclear astrophysics. According to the baryon density determined by Wilkinson microwave anisotropy probe (WMAP)[1], the primary abundances for ^{6}Li and ^{7}Li predicted by standard BBN (SBBN) model deviate clearly from the observations of the metal-poor halo stars[2], where the lithium abundances exhibit a "plateau" behavior[3]. Several investigations for both astrophysical observation and nucleosynthesis calculation have been attempted to explain the large discrepancies, but none of them has been successful up to now. In addition, due to the difference between the depletion speeds of ^{6}Li and ^{7}Li in stars, the ^{6}Li/^{7}Li ratio could stand for a measure of the time scale for stellar evolution. In the above scenario, ^{6}Li(n,γ)^{7}Li is believed to be one of the important reactions in the SBBN network[4, 5], its reaction rates would affect the abundances of both ^{6}Li and ^{7}Li.

The cross sections of ^{6}Li(n,γ)^{7}Li at astrophysically relevant energies are most likely dominated by the E1 transitions into the ground and first exited states in ^{7}Li. To date, only one direct measurement of the ^{6}Li(n,γ)^{7}Li cross sections at stellar energies has been performed[6]. The cross sections can also be calculated by the direct capture model with the spectroscopic factors of ^{7}Li=^{6}Li⊗n extracted from the neutron transfer reactions. In the previous studies, the spectroscopic factors were mostly derived by ^{6}Li(d, p)^{7}Li and ^{7}Li(p, d)^{6}Li reactions[7–11], the results are correlative with the neutron spectroscopic factor of deuteron. Thus, it is highly desired to extract the spectroscopic factors through a self-contained reaction without third-participant, which can provide an independent verification.

The elastic-transfer reaction is a good tool to extract the single nucleon spectroscopic factors, which has been used to determine the spectroscopic factor of ^{9}Be=^{8}Li⊗p with ^{9}Be(^{8}Li,^{9}Be)^{8}Li reaction[12]. In such an approach, the events from elastic scattering and elastic-transfer reaction can not be distinguished, but the theoretical calculation shows that their mutual contributions at the respective forward angles are negligibly small. As a result, the effective differential cross sections at forward angles of the two processes can be obtained respectively. The obvious advantages of this approach are (i) the elastic scattering and elastic-transfer reaction have the same entrance and exit channels, the spectroscopic factor can be derived by one set of optical potential deduced from the elastic scattering and (ii) the elastic-transfer reaction does not involve third participant in the entrance and exit channels, and thus conduces to the reduction of experimental result uncertainty.

For the above reasons, we chose the ^{7}Li(^{6}Li,^{7}Li)^{6}Li elastic-transfer reaction to extract the spectroscopic factors of the ^{7}Li=^{6}Li⊗n. This reaction has been measured in 1998 at E$_{lab}$=9-40 MeV[13], unfortunately the minimum angle reached in that experiment was about 30° in the center of mass frame (for transfer process), that was not suitable to derive the spectroscopic factor. In present work, we have measured the angular distributions of the ^{7}Li(^{6}Li,^{6}Li)^{7}Li elastic scattering and ^{7}Li(^{6}Li,^{7}Li$_{g.s.}$)^{6}Li, ^{7}Li(^{6}Li,^{7}Li$_{0.48}$)^{6}Li transfer reactions at E$_{c.m.}$=23.7 MeV. The neutron spectroscopic factors for the ground and first exited states in ^{7}Li were determined by comparing the experimental results with the distorted-wave Born approximation (DWBA) calculations, and then used to calculate the cross sections and astrophysical rates of ^{6}Li(n,γ)^{7}Li direct capture reaction.

The experiment was carried out at the Beijing HI-13 tandem accelerator. A 44 MeV ^{6}Li beam in intensity of about 100 pnA impinged on the natural LiF target in thickness of 530 $\mu g/cm^2$, which was evaporated on a 50 $\mu g/cm^2$ carbon foil. The beam was collected by a Fara-

*Supported by the the National Basic Research Programme of China under Grant No. 2007CB815003, the National Natural Science Foundation of China under Grant Nos.10675173, 10720101076, 10735100 and 10975193.
†Electronic address: junsu@iris.ciae.ac.cn

day cup behind the target for counting the number of ^{6}Li. The Faraday cup covered an angle range of $\pm 6^\circ$ and confined the attainable minimum angle in the measurement. The reaction products were focused and separated by Q3D magnetic spectrograph. The accepted solid angle of Q3D was set to be 0.23 mSr for a better angular resolution. A two-dimensional position sensitive silicon detector (PSSD) was set at the focal plane of Q3D, the X-Y information from PSSD enabled the products emitted into the accepted solid angle of Q3D to be fully recorded, and the corresponding energy signals were used to remove the impurities with the same magnetic rigidity. The absolute differential cross sections were determined by normalizing the measurements of the ^{7}Li(^{6}Li,^{6}Li)^{7}Li elastic scattering and the ^{7}Li(^{6}Li,^{7}Li$_{g.s.}$)^{6}Li, ^{7}Li(^{6}Li,^{7}Li$_{0.48}$)^{6}Li transfer reactions to the elastic scattering of ^{6}Li on the gold target at $\theta_{lab} = 25^\circ$.

The experiment setup was tested beforehand by measuring the angular distribution of ^{12}C(^{7}Li,^{7}Li)^{12}C elastic scattering at E$_{lab}$=36 MeV. As shown in the Fig. 1, our result is in fair agreement with that reported in Ref.[14], indicating a reliable overall performance of our setup and data analysis procedure.

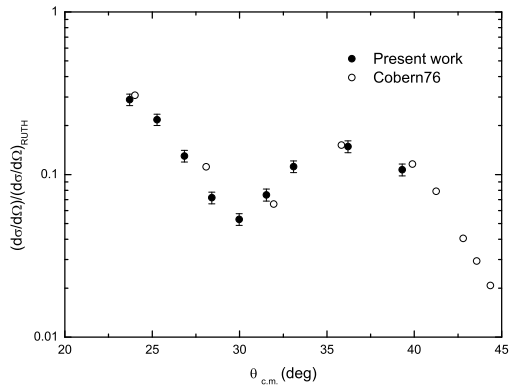

FIG. 1: Comparison of the ^{12}C(^{7}Li,^{7}Li)^{12}C angular distributions at E$_{lab}$=36 MeV, the solid and open circles denote the data obtained in the present experiment and an earlier work[14], respectively.

In the measurements of ^{7}Li(^{6}Li,^{6}Li)^{7}Li elastic scattering and ^{7}Li(^{6}Li,^{7}Li$_{g.s.}$)^{6}Li, ^{7}Li(^{6}Li,^{7}Li$_{0.48}$)^{6}Li transfer reactions, the magnetic fields of Q3D were set to focus ^{6}Li and ^{7}Li, respectively. The elastic scattering and transfer processes were measured in the angular ranges of $7^\circ \leq \theta_{lab} \leq 30^\circ$ and $7^\circ \leq \theta_{lab} \leq 17^\circ$ in steps of 1°, respectively.

The differential cross sections for elastic scattering are shown in the Fig. 2, with uncertainties from the errors of statistics and target thickness. The angular distribution of ^{7}Li(^{6}Li,^{6}Li)^{7}Li elastic scattering was analyzed by employing the code PTOLEMY[15] and optical model using real and imaginary potentials with Woods-Saxon form . The optimized potential parameters obtained by fitting the experimental data are listed in the Table I. The fitting results are shown in Fig. 2 with the experimental data. Fig. 2 also exhibits the contribution of transfer processes, which is less than 1% in the experimental angular range.

TABLE I: Optical potential parameters of ^{6}Li+^{7}Li at E$_{c.m.}$=23.7 MeV. The depths and geometrical parameters are in MeV and fm, respectively.

U_V	r_R	a_R	W_V	r_I	a_I	r_c	$\chi^2/point$
73.4	0.5	0.92	32.6	1.0	0.8	1.25	4.0

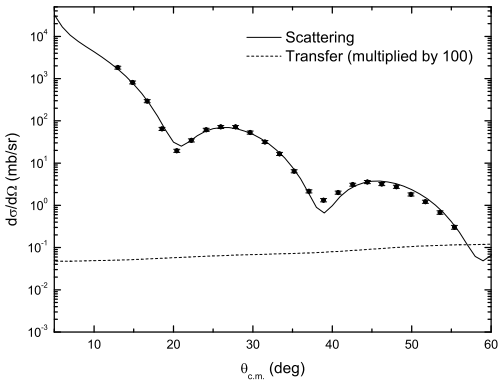

FIG. 2: Differential cross sections for ^{7}Li(^{6}Li,^{6}Li)^{7}Li elastic scattering at E$_{c.m.}$=23.7 MeV together with the optical model calculation. The dashed line denotes the contribution of transfer processes (multiplied by a factor of 100).

The angular distributions of ^{7}Li(^{6}Li, ^{7}Li$_{g.s.}$)^{6}Li and ^{7}Li(^{6}Li, ^{7}Li$_{0.48}$)^{6}Li transfer processes are shown in Fig. 3, which were also analyzed with the code PTOLEMY. As can clearly be seen from Fig. 3, the contribution of elastic scattering is negligible small. In the calculation, we utilized the ^{6}Li+^{7}Li optical potential parameters listed in Table I for both the entrance and exit channels. For the bound states, a Woods-Saxon potential with the standard geometrical parameters r_0=1.25 fm and a=0.65 fm was adopted and the depths were adjusted to reproduce the neutron binding energies of ^{7}Li.

The spectroscopic factor ^{7}Li=^{6}Li$\otimes$n, denoted as S$_{^7Li}$, can be derived by normalizing the DWBA calculations to the experimental data according to the expression

$$(\frac{d\sigma}{d\Omega})_{EXP} = S^2_{^7Li}(\frac{d\sigma}{d\Omega})_{DWBA}. \quad (1)$$

Generally, the experimental data in the first peak of angular distributions at the forward angles are suitable for extracting the spectroscopic factor[16] because the differential cross sections of other angles are more sensitive to some high-order processes. In our calculation, only the first three data at the forward angles were used to extract

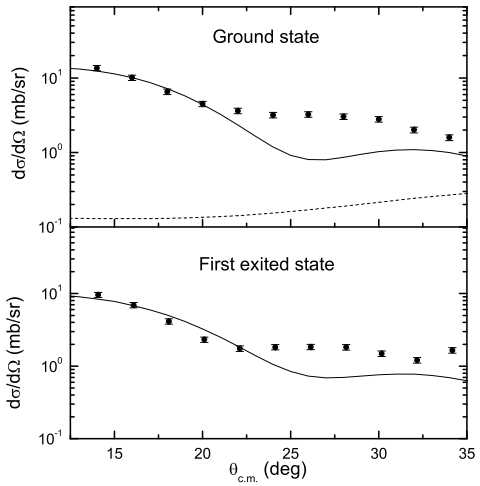

FIG. 3: Angular distribution of ^{7}Li(^{6}Li, ^{7}Li$_{g.s.}$)^{6}Li and ^{7}Li(^{6}Li, ^{7}Li$_{0.48}$)^{6}Li at E$_{c.m.}$=23.7 MeV together with the DWBA calculations normalized to the first three data at forward angles. The dash line denotes the contribution of elastic scattering (multiplied by a factor of 1000).

the spectroscopic factors. For the ^{7}Li(^{6}Li, ^{7}Li$_{g.s.}$)^{6}Li channel, both of the neutron transfers to the 1p$_{3/2}$ and 1p$_{1/2}$ orbits of ^{7}Li were taken into account, consequently the result was the coherent sum of their contributions. Since the 1p$_{3/2}$ and 1p$_{1/2}$ components can not be distinguished experimentally, their ratio was taken to be 1.5 based on the calculation[17], then the spectroscopic factor of ^{7}Li$_{g.s.}$ =^{6}Li⊗n was determined to be 0.73 ± 0.05, the uncertainty results from the measurement, scattering potential fitting and the divergence of the values derived from three different angles. For the first exited state in ^{7}Li, only the neutron transfer to the 1p$_{3/2}$ orbit was considered because the contribution of 1p$_{1/2}$ orbit is merely about 4%[17], then the spectroscopic factor of ^{7}Li$_{0.48}$ =^{6}Li⊗n was derived to be 0.90 ± 0.09. The spectroscopic factors obtained in several theoretical and experimental investigations are listed in Table II, our results agree well with the theoretical calculation[17–20] and the experimental data[8, 9].

At low energies of astrophysical interest, the ^{6}Li(n,γ)^{7}Li direct capture cross sections are dominated by the E1 transition from incoming s-wave to the bound state, the contribution of d-wave neutrons is negligible. In the computation we used the code RADCAP[21] and Woods-Saxon form potential with the standard geometrical parameters. The potential depths of the ^{7}Li bound states were adjusted to reproduce the neutron binding energies of its ground and first excited states, respectively. For the scattering potential, the depth can be fixed by fitting the well measured ^{6}Li(p,γ)^{7}Be cross sections at low energies[22] because the difference between n+^{6}Li and p+^{6}Li potentials is only a Coulomb modification of depth, which is given by $\Delta V = 0.4Z/A^{1/3}$[23].

TABLE II: The theoretical and experimental neutron spectroscopic factors for the ground and first exited states in ^{7}Li.

$S_{^7Li_{g.s.}}$	$S_{^7Li_{0.48}}$	Experiments or theory	Reference
0.72	0.89	theory	[17]
0.80	0.98	theory	[18]
0.79	0.97	theory	[19]
0.77	1.07	theory	[20]
0.90	1.15	^{6}Li(d,p)	[7]
0.71		^{7}Li(p,d)	[8]
0.72 ± 0.1		^{7}Li(p,d)	[9]
0.87		^{7}Li(p,d)	[10]
1.85 ± 0.37		^{6}Li(d,p)	[11]
0.73 ± 0.05	0.90 ± 0.09	^{7}Li(^{6}Li,^{7}Li)	present work

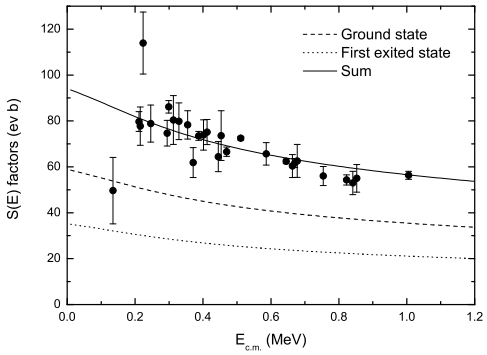

FIG. 4: Astrophysical S(E) factors of the ^{6}Li(p,γ)^{7}Be reaction. The experimental data are taken from Ref.[22].

The ^{6}Li(p,γ)^{7}Be cross sections were also calculated by the same code. The neutron spectroscopic factors of ^{7}Li derived above were correspondingly taken as the proton spectroscopic factors for the ground and first exited states in ^{7}Be owing to the charge symmetry. Here, the depth of scattering potential was constrained to be 41.3 ± 2.0 MeV in reproducing the experimental data. The calculated astrophysical ^{6}Li(p,γ)^{7}Be S(E) factors are shown in Fig. 4 together with the experimental results. In addition to a good agreement between the calculated and measured total S(E) factors, our calculation also indicates that the contributions of ground and first exited states are about 63% and 37%, respectively, which are very close to the experimental values 61% and 39%[22].

Considering the Coulomb modification, the scattering potential depth of n+^{6}Li was chosen to be 40.6 ± 2.0 MeV. Then the ^{6}Li(n,γ)^{7}Li$_{g.s.}$ and ^{6}Li(n,γ)^{7}Li$_{0.48}$ cross sections were calculated using the spectroscopic factors and optical potentials extracted above, and compared with the experimental data[6], as shown in Fig. 5. Our result is consistent with the direct measurement, showing an approximate 1/v behavior, so that the reaction rates are almost constant at energies of astrophysical interest.

The astrophysical ^{6}Li(n,γ)^{7}Li direct capture reaction

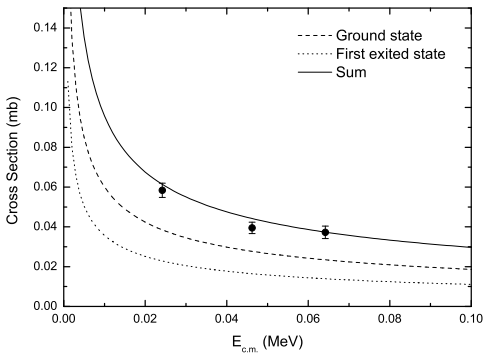

FIG. 5: Cross sections of the ^{6}Li(n,γ)^{7}Li reaction. The experimental data are taken from Ref.[6].

rate was then calculated by the expression[24]

$$N_A\langle\sigma v\rangle = 3.73\times10^{10}A^{-\frac{1}{2}}T_9^{-\frac{3}{2}}\int_0^\infty \sigma E exp(\frac{-11.6E}{T_9})dE, \quad (2)$$

where A is the reduced mass in amu, T_9 is the temperature in units of 10^9K. E, σ and reaction rate are given in MeV, barns and cm^{3}mol^{-1}s^{-1}, respectively. The reaction rate was found to be $(8.5\pm1.7)\times10^3$ cm^{3}mol^{-1}s^{-1}, the error results from the uncertainties of spectroscopic factors and scattering potential depth.

Summarizing, the measurements of differential cross sections for the ^{7}Li(^{6}Li,^{6}Li)^{7}Li elastic scattering and ^{7}Li(^{6}Li,^{7}Li$_{g.s.}$)^{6}Li, ^{7}Li(^{6}Li,^{7}Li$_{0.48}$)^{6}Li transfer reactions have been carried out at E$_{c.m.}$=23.7 MeV, in which the angular distributions for transfer processes were obtained in the range of $14^\circ \lesssim \theta_{c.m.} \lesssim 34^\circ$ for the first time. By using the optical potential of ^{6}Li+^{7}Li extracted from the elastic scattering, the spectroscopic factors of ^{7}Li=^{6}Li$\otimes$n were deduced with DWBA analysis, the results are in agreement with those reported previously[8, 9, 17–20]. Then the ^{6}Li(n,γ)^{7}Li direct capture cross sections have been derived and compared with the direct measurement data. The astrophysical reaction rate was found to be higher by a factor of 1.7 than the value adopted in previous reaction network calculations[4, 5].

[1] Dunkley J et al 2009 *Astrophys. J. Suppl* **180** 306
[2] Cayrel R et al 2008 *arXiv:0810.4290v2*
[3] Spite F and Spite M 1982 *Astronomy and Astrophysics* **115** 357
[4] Malaney R A and Fowler W A 1989 *Astrophys. J.* **345** L5
[5] Nollett K M, Lemoine M and Schramm D N 1997 *Phys. Rev. C* **56** 1144
[6] Toshiro O et al 2000 *AIP Conference Proceedings* **529** 678
[7] Schiffer J P et al 1967 *Phy. Rev.* **164** 1274
[8] Li T Y and Mark S K 1969 *Nucl. Phys. A* **123** 147
[9] Towner I S 1969 *Nucl. Phys. A* **126** 97
[10] Fagerström B et al 1976 *Phys. Scr* **13** 101
[11] Tsang M B, Lee J and Lynch W G 2005 *Phys. Rev. Lett.* **95** 222501
[12] Camargo O et al 2008 *Phys. Rev. C* **78** 034605
[13] Potthast K W et al 1998 *Nucl. Phys. A* **629** 656
[14] Cobern M E, Pisano D J and Parker P D 1976 *Phys. Rev. C* **14** 491
[15] Macfarlane M H and Pieper S C 1976 *Argonne Nat. Lab. Report* No. ANL-76-11 (unpublished)
[16] Liu X D et al 2004 *Phys. Rev. C* **69** 064313
[17] Cohen S and Kurath D 1967 *Nucl. Phys. A* **101** 1
[18] Barker F C 1966 *Nucl. Phys. A* **83** 418
[19] Varma S and Goldhammer P 1969 *Nucl. Phys. A* **125** 193
[20] Kumar N 1974 *Nucl. Phys. A* **225** 221
[21] Bertulani C A 2003 *Comput. Phys. Commun.* **156** 123
[22] Switkowski Z E et al 1979 *Nucl. Phys. A* **331** 50
[23] Dave J H and Gould C R 1983 *Phys. Rev. C* **28** 2212
[24] Angulo C 1999 *Nucl. Phys. A* **656** 3